



ORIGINAL ARTICLE

Digital next-generation sequencing of cell-free DNA for pancreatic cancer

Shinichi Takano,  Mitsuharu Fukasawa, Hiroko Shindo, Ei Takahashi, Yoshimitsu Fukasawa, Satoshi Kawakami, Hiroshi Hayakawa, Natsuhiko Kuratomi, Makoto Kadokura, Shinya Maekawa  and Nobuyuki Enomoto

First Department of Internal Medicine, Faculty of Medicine, University of Yamanashi, Chuo, Japan

Key words

cell-free DNA, liquid biopsy, next-generation sequencing, pancreatic ductal carcinoma.

Accepted for publication 8 March 2021.

Correspondence

Shinichi Takano, First Department of Internal Medicine, Faculty of Medicine, University of Yamanashi, 1110 Shimokato, Chuo, Yamanashi 409-3898, Japan.
Email: stakano@yamanashi.ac.jp

Declaration of conflict of interest: None

Funding support: Japan Society for the Promotion of Science15K0904418K0799919K08418

Abstract

Background and Aim: The clinical applicability of digital next-generation sequencing (dNGS), which eliminates polymerase chain reaction (PCR) and sequencing error-derived noise by using molecular barcodes (MBs), has not been fully evaluated. We evaluated the utility of dNGS of cell-free DNA (cfDNA) in liquid biopsies obtained from patients with pancreatic cancer.

Methods: Fifty-eight patients with pancreatic cancer undergoing endoscopic ultrasound-guided fine-needle aspiration (EUS-FNA) were included. Samples were subjected to sequencing of 50 cancer-related genes using next-generation sequencing (NGS). The results were used as reference gene alterations. NGS of cfDNA from plasma was performed for patients with a mutant allele frequency (MAF) >1% and an absolute mutant number > 10 copies/plasma mL in *KRAS* or *GNAS* by digital PCR. Sequence readings with and without MBs were compared with reference to EUS-FNA-derived gene alterations.

Results: The concordance rate between dNGS of cfDNA and EUS-FNA-derived gene alterations was higher with than without MBs ($p = 0.039$), and MAF cut-off values in dNGS could be decreased to 0.2%. dNGS using MBs eliminated PCR and sequencing error by 74% and 68% for *TP53* and all genes, respectively. Overall, dNGS detected mutations in *KRAS* (45%) and *TP53* (26%) and copy number alterations in *CCND2*, *CCND3*, *CDK4*, *FGFR1*, and *MYC*, which are targets of molecular-targeted drugs.

Conclusions: dNGS of cfDNA using MBs is useful for accurate detection of gene alterations even with low levels of MAFs. These results may be used to inform the development of diagnostics and therapeutics that can improve the prognosis of pancreatic cancer.

Introduction

Pancreatic cancer is a dismal disease with a 5-year survival rate of <5% in the United States¹ and 4.7% in Japan.² The poor prognosis reflects difficulties with detecting early stages of the disease, and efficient therapies are limited. Recently, new therapies for unresectable tumors, such as molecular-targeted therapies and immunotherapies, have gained attention³; however, the number of molecular-targeted drugs or immune checkpoint inhibitors for pancreatic cancer treatment is limited, and these drugs are only effective in a minor proportion of pancreatic cancer. Therefore, a precision medicine that provides the best therapy to the individual patient with pancreatic cancer according to the tumor genetic profile is urgently needed.

Endoscopic ultrasound-guided fine-needle aspiration (EUS-FNA) is typically used to obtain tumor tissue from pancreatic cancer.⁴ It is an invasive procedure and is impractical to

repeat each time the tumor progresses. Meanwhile, liquid biopsy enables the identification of tumor genetic abnormalities in body fluids, such as plasma, serum, and urine. Liquid biopsy is a minimally invasive method for obtaining genetic profiles using cell-free DNA (cfDNA),^{5–7} circulating tumor cells,^{8–10} and microRNA.^{11–13} Liquid biopsy may be clinically applicable to early tumor detection,^{14,15} tumor monitoring,^{16–20} treatment effect prediction,¹⁶ detection of drug resistance, and as a sensitive tumor marker^{14,17,21–24} because of its advantages. However, the sensitivity of cfDNA-based tumor mutation detection is currently reported to be 51–97% and 35–86% using digital polymerase chain reaction (dPCR)^{8,14,15,20–23,25} and next-generation sequencing (NGS),^{15,18,19,24,26,27} respectively. Although NGS can detect several genetic abnormalities in a single assay, the sensitivity of NGS in terms of detecting mutations is lower than that of dPCR owing to sequencing errors in NGS. Meanwhile, various technical adjustments have improved liquid biopsy sensitivity, such as

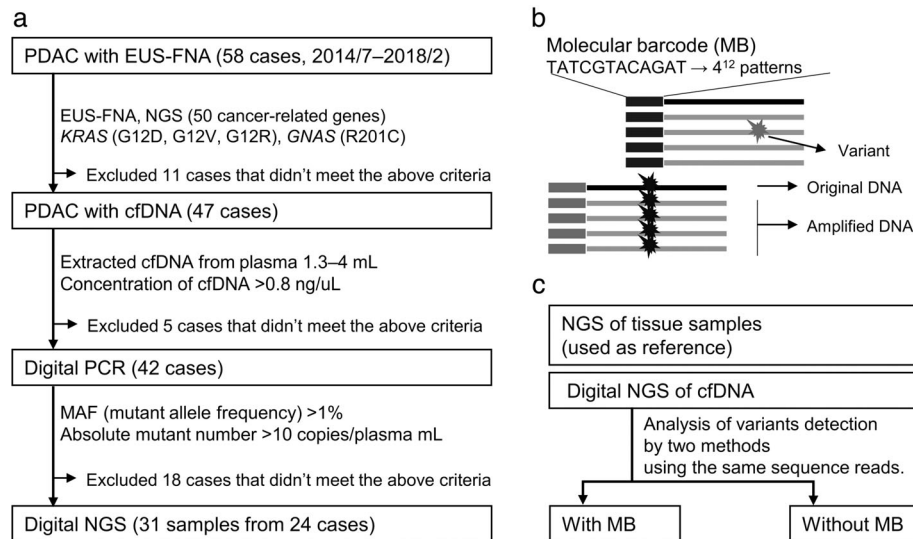


Figure 1 Flow chart of this study. (a) Selection of patients and samples in this study. (b) A schema describing digital next-generation sequencing (dNGS) using molecular barcodes (MBs). (c) The flow of the NGS analyses.

enrichment with methylated cfDNA,²⁸ enrichment with fractionated small cfDNA,^{29,30} preamplification of target genes,^{31,32} and molecular barcoding of DNA.^{33–36} Among these, NGS with molecular barcodes (MBs), also known as digital NGS (dNGS), reduces PCR or sequence errors and enables the detection of rare mutations, even in cfDNA samples.

Because tumor genetic profiles can easily and repeatedly be made available to inform the best choice of treatments, liquid biopsy is an attractive monitoring method for pancreatic cancer. However, the sensitivity of dNGS for liquid biopsy might not be sufficiently high, and the genetic profile identified in the liquid biopsy might not correspond with that in tumor tissue. Therefore, this study aimed to evaluate the accuracy of dNGS-based liquid biopsy by comparing sequence read analysis with and without MB and by comparing mutations identified using liquid biopsy with tissue mutations.

Methods

Patients and tissue samples. We retrospectively reviewed the medical records of 58 patients with pancreatic cancer who underwent EUS-FNA at Yamanashi University Hospital between July 2014 and February 2018. Tissue samples obtained by EUS-FNA were available as formalin-fixed paraffin-embedded (FFPE) block-derived 8 μ m-thick sections, from which tumor components were separated by laser capture microdissection (LCM) using an ArcturusXT Laser Capture Microdissection System (Life Technologies, Carlsbad, CA, USA). DNA extraction from specimens obtained from LCM was performed as previously reported.³⁷ DNA from biopsied specimens was extracted using the GeneRead DNA FFPE Kit (QIAGEN, Hilden, Germany) according to the manufacturer's specifications. The quantity and quality of extracted DNA were evaluated using a NanoDrop instrument (Thermo Fisher, Waltham, MA, USA) with the Qubit platform (Thermo Fisher Scientific). The

distribution of samples is shown in the flow chart in Figure 1a. This study was approved by the Human Ethics Review Committee of Yamanashi University Hospital (Receipt numbers 1326 and 1847). Research data obtained in this study are not shared.

Genetic mutational analysis of tissue samples.

Genetic analysis of tumor specimens was performed by amplifying the extracted DNA (10 ng) using barcode adaptors (Ion Xpress Barcode Adapters 1-96 Kit, Life Technologies) with the Ion AmpliSeq Cancer Hotspot panel v.2 (Thermo Fisher Scientific), which contains 207 primer pairs and targets approximately 2800 hotspot mutations in 50 cancer-related genes from the COSMIC database³⁸ (Table S1, Supporting information). Barcoded libraries were amplified using emulsion PCR on Ion Sphere particles, and sequencing was performed on an Ion Chef System and an Ion Proton Sequencer (Life Technologies) using the Ion PI Hi-Q Chef Kit (Life Technologies). Variants were identified using the Ion reporter software v. 5.10 (Thermo Fisher Scientific). Furthermore, and to avoid false-positive variants due to sequencing errors, only variants with a mutant allele frequency (MAF) of $>4\%$ (with a sequence read depth of >100) were considered to be valid in tissue samples.

Extraction of cfDNA from plasma samples. A total of 65 blood samples were obtained from the 58 patients before and during treatment. Furthermore, multiple blood samples were obtained during systemic chemotherapy from five patients. The blood samples were collected in BD Vacutainer[®] CPT[™] tubes (Becton Dickinson, NJ, USA) containing 0.1 M sodium citrate solution as an anticoagulant, and the tubes were processed according to the manufacturer's instructions. After being inverted carefully four times, the CPT tubes were centrifuged at 1800g for 20 min at room temperature, from which plasma was collected from the uppermost layer and stored within 3 h of blood collection at -20°C until use. CfDNA was extracted from

Table 1 Patient characteristics

| Characteristics | | Value (<i>n</i> = 24) |
|---|--------------------------|------------------------|
| Age | Median (range) | 65.5 (44–84) |
| Gender | M/F | 11/13 |
| Location | Ph/Pbt | 10/14 |
| Tumor stage, <i>n</i> (%) | II | 6 (25) |
| | III | 4 (17) |
| | IV | 14 (58) |
| Therapy, <i>n</i> (%) | BSC | 1 (4) |
| | Chemotherapy | 22 (92) |
| | Operation | 1 (4) |
| <i>KRAS</i> mutation, [†] <i>n</i> (%) | G12D | 8 (33) |
| | G12V | 11 (46) |
| | G12R | 4 (17) |
| | WT (<i>GNAS</i> _R201C) | 1 (4) |

[†]EUS-FNA sample.

BSC, best supportive care; EUS-FNA, endoscopic ultrasound-guided fine-needle aspiration; Ph, pancreatic head; Pbt, pancreatic body and tail.

between 1.3 and 4.0 mL of plasma with the QIAamp Circulating Nucleic Acid Kit (QIAGEN) and with the QIAvac 24 Plus vacuum manifold. Carrier RNA was added to the ACL lysis buffer to enhance the binding of nucleic acids to the QIAamp membrane and hence enhance the respective yields. The size and concentrations of cfDNA were subsequently measured using the High Sensitivity DNA Kit (Agilent, Santa Clara, CA, USA) using Agilent 2100 Bioanalyzer on-chip electrophoresis.

dPCR analyses. dPCR was performed on a QuantStudio™ 3D Digital PCR System platform consisting of a Gene Amp 9700 PCR machine (including a chip adapter kit), an automatic chip loader, and the QuantStudio™ 3D Instrument (Thermo Fisher Scientific). Consequently, the collected data were analyzed with QuantStudio 3D AnalysisSuite Cloud Software (Thermo Fisher Scientific). Mutation analysis of cfDNA by dPCR was based on a 5'-exonuclease assay using TaqMan®-MGB probes targeting *KRAS* G12V, G12D, G12R, and *GNAS* R201C (Thermo Fisher Scientific, Catalog number: A44177), which were chosen according to the genetic profiles observed in tissue samples.

dNGS analyses. dNGS analysis of cfDNA was performed by amplifying the extracted DNA with RNA (up to 20 ng) using the OncoPrint™ Pan-Cancer Cell-Free Assay (Thermo Fisher Scientific), which targets mutations and short indels in 52 genes with 272 primer pairs as shown in Table S2, including copy number variations (CNVs) and fusions in 12 genes. DNAs were coupled to dual barcodes, which consist of sequences of 12 randomly arranged nucleotides (MBs) for tag sequence and sample barcodes, during the first PCR, using the Tag Sequencing Barcode Set (Thermo Fisher Scientific, Fig. 1b). Sequencing of barcoded libraries was performed on an Ion Chef System and an Ion Proton Sequencer (Life Technologies) using the Ion PI Hi-Q Chef Kit (Life Technologies) as described above.

Obtained sequence reads were analyzed with and without MBs for comparison using the Ion reporter software v. 5.10

(Fig. 1C). Hence, dNGS analysis taking MBs into account (which reduces erroneous sequence reads by eliminating inconsistent mutations in sequence reads with the same MB) was compared with ordinary NGS analysis (i.e. NGS analysis not taking MBs into account).

Statistical analysis. All mutations detected in cfDNA were compared with those detected in tissues to evaluate whether the mutations detected in cfDNA matched those in tumor tissue samples. The match rates between cfDNA-derived mutations and tissue-derived mutations were compared between the analyses with and without MBs through the analysis of receiver operating characteristics (ROC) using the DeLong test.

Factors associated with successful mutation detection in cfDNA were identified by the Wilcoxon rank sum test and logistic regression analysis for univariate and multivariate analyses, respectively, and were considered statistically significant when probability (*P*) values were <0.05. All statistical analyses were performed using R (version 3.6.0).

Results

Patient characteristics and qualitative assessment of extracted DNA. Figure 1a depicts the flow chart of the study. Finally, a total of 31 samples from 24 patients with pancreatic ductal adenocarcinoma who underwent EUS-FNA between July 2014 and February 2018 were included in the study after excluding 11, 5, and 18 patients from 58 patients due to lack of mutations in either *KRAS* or *GNAS* by NGS analysis in tissue samples, <0.8 ng/uL cfDNA concentration, and MAF and absolute mutant number by dPCR using cfDNA extracted from plasma samples of <1% and 10 copies/plasma mL, respectively. Table 1 shows the clinical characteristics of all 24 patients, 14 (58%) of whom were in stage IV, and 22 patients (92%) received chemotherapy. The proportion of cases with *KRAS* G12D, G12V, G12R, and *GNAS* R201C mutations detected in tissues obtained by EUS-FNA was 33%, 46%, 17%, and 4%, respectively.

The mean (\pm standard deviation [SD]) and median (range) quantities of extracted DNA from FPPE samples obtained by EUS-FNA were 32.3 ng (\pm 58.1) and 12.9 ng (1.5–228), respectively, while those of extracted cfDNA from 1.3–4 mL of plasma were 19.3 ng (\pm 2.5) and 20 ng (8.4–20), respectively. In the NGS analyses of tissue samples obtained by EUS-FNA, the target regions of 50 cancer-related genes included 22 027 bases, and the average (\pm SD) and median (range) sequence read depths were 4625 (\pm 2630) and 4272 (1212–11 159), respectively. In addition, with regard to dNGS analyses of cfDNA, target regions of 52 cancer-related genes included 14 774 bases, and the mean (\pm SD) sequence read depth and molecular depth, indicating the number of unique MBs, were 18 509 (\pm 14 006) and 793 (\pm 773), respectively (Table S3).

Comparison of mutations detected in cfDNA with and without MB analysis and in tissue samples. Mutations detected by NGS in EUS-FNA tissue samples and plasma-derived cfDNA samples are shown in Figure 2. The four most frequent mutations in tissue samples were identified in *KRAS* (97%), *TP53* (65%), *SMAD4* (10%), and *STK11* (10%).

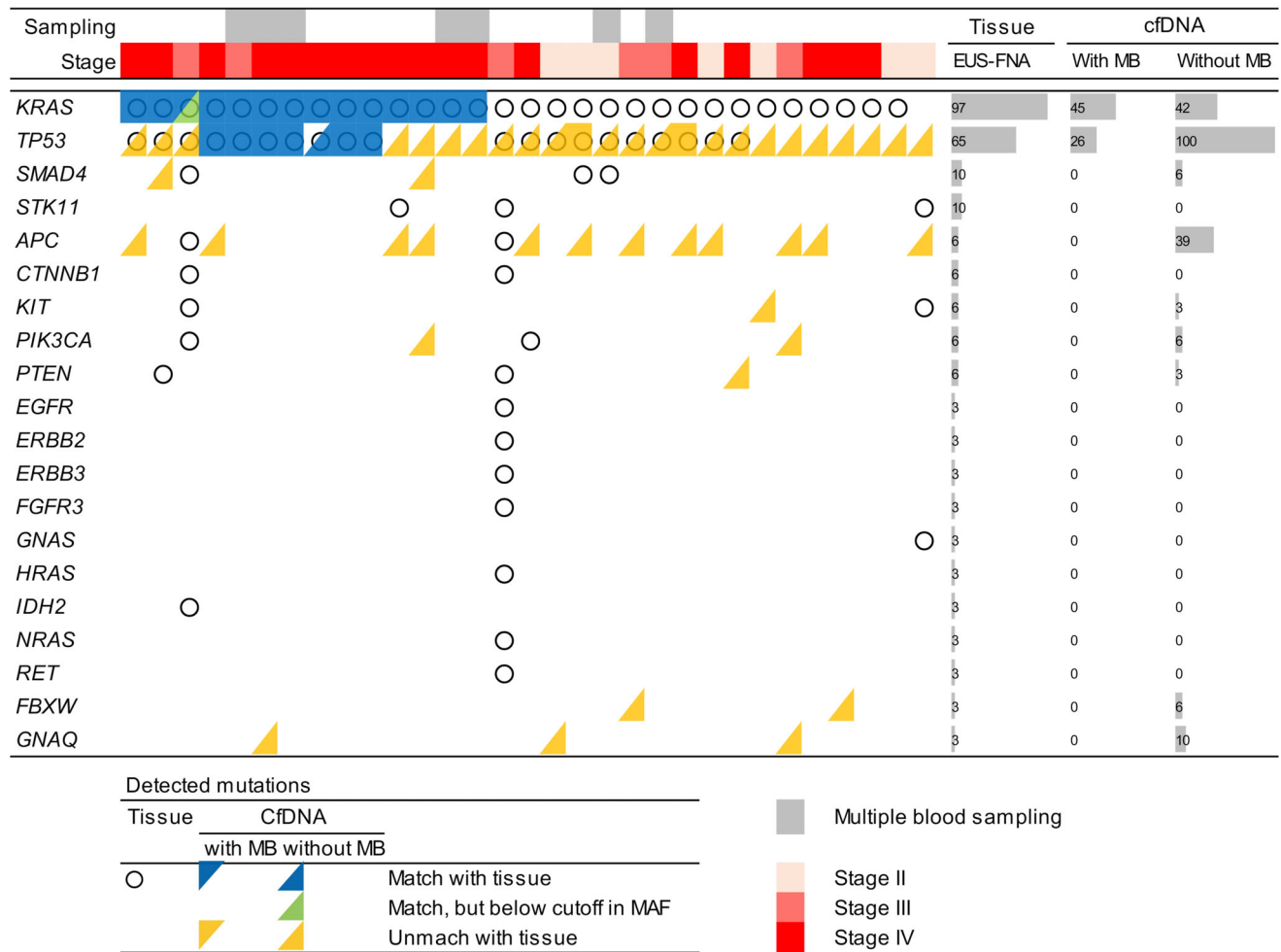


Figure 2 Mutations detected in tissue samples and cell-free DNA obtained by liquid biopsy by DNA-based analyses with and without molecular barcodes (MB). The panel provides a summary of mutations detected in tissue samples and cfDNA. The boxes in the middle panel represent detected mutations in each case, in which a circle, an upper left triangle, and a lower right triangle represent mutations in tissue, cfDNA with MB, and cfDNA without MB, respectively. Blue and yellow triangles represent cfDNA-derived mutations that matched or did not match tissue-derived mutations. The light green triangle in *KRAS* was a cfDNA mutation, which matched a tissue mutation, although its mutant allele frequency (MAF) was lower than the cut-off value. The left side of the panel displays the gene symbols, and the frequencies of mutation in each gene are shown in the right side of the panel. The upper side of the panel shows the clinical stages of each case and cases of multiple sampling (gray case), in which multiple cfDNA samples were obtained at different times. cfDNA, cell-free DNA; EUS-FNA, endoscopic ultrasound-guided fine-needle aspiration; MB, analyses using molecular barcodes.

Mutations detected in cfDNA were analyzed by two methods, mutation detection analysis with and without MB. Because variants detected by NGS contain many sequencing- and/or PCR-derived errors, we compared variants detected in cfDNA with those in tissue samples that were considered most reliable among the obtained genetic profiles. When including valid mutation variants in tissue samples, the match rate of cfDNA-derived mutations with tissue-derived mutations was higher in analyses considering MB than in those that did not consider MB as evaluated by ROC analysis with an area under the curve of 0.89 and 0.84 ($P = 0.039$, Fig. 3a), respectively. When MAF cut-off values were set at 0.2% and 0.5% in the analyses with and without MB, respectively, the match rates of cfDNA mutations with

tissue mutations were 78.6% and 78.6%, respectively, with the mismatch rate being 18.2% in the analysis without MB. When the cut-off value of MAF was set at 10% in the analysis without MB, the match rate and mismatch rate of cfDNA mutations with tissue mutations were 17.9% and 0%, respectively (Fig. 3b, Table 2).

Overview of gene alterations of cfDNA detected by dNGS. Based on the cut-off value established in the previous section, an overview of all the gene alterations of cfDNA detected by dNGS is provided in Table 3. Among the 31 samples from the 24 patients, mutations in *KRAS* and *TP53* were detected in 14 (45%) and 8 (26%) samples, respectively, with MAFs as

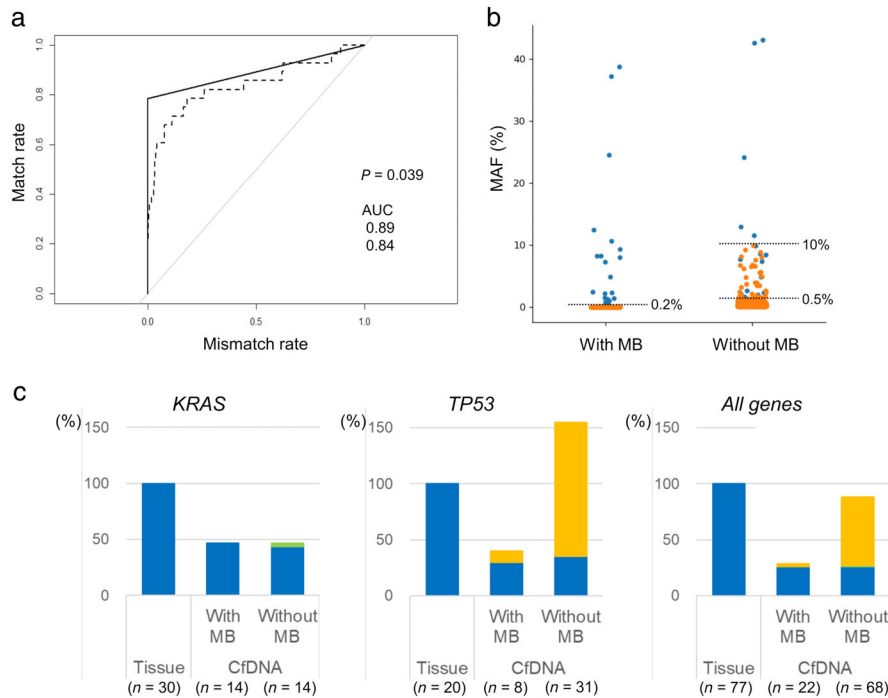


Figure 3 Mutant allele frequencies (MAFs) and numbers of detected mutations of cell-free DNA (cfDNA) analyzed by with and without molecular barcodes (MBs). (a) The cut-off value of (MAFs) in the cfDNA-derived mutation that matched with the tissue-derived mutation was evaluated by receiver operating characteristics (ROC) curve analysis. The area under the curve was 0.89 and 0.84 ($p = 0.039$) in analyses with and without MB, respectively. —, With MB; ----, without MB. (b) MAF plots of detected mutations in cfDNA by next-generation sequencing (NGS) analyses with and without MB. Matches and mismatches with mutations detected in tissue samples are shown in blue and orange dots, respectively. Cut-off values for matched mutations (i.e. same mutations in cfDNA and tissue samples) were determined by ROC curve analysis to be 0.2% and 0.5% by dNGS and ordinary NGS, respectively. The sensitivity and specificity for matched mutations were 83.3% and 93.3% by dNGS, respectively, and 73.9% and 92.9% by ordinary NGS, respectively. ●, Match; ●, mismatch. (c) The proportion of concomitant cfDNA with tissue mutations in *KRAS*, *TP53*, and all assayed genes. The number of mutations detected in tissue samples are shown in the left in each graph, and cfDNA mutations matching with those identified in tissue samples are shown in bar plots. Tissue-matched and -mismatched cfDNA mutations are shown as blue and yellow bars, respectively, whereas tissue-matched mutations with a lower MAF than the cut-off value are shown as light green bars. ■, Mismatch; ■, match < cutoff; ■, match or tissue. MAF, mutant allele frequency; MB, dNGS analysis with molecular barcodes; cfDNA, cell-free DNA.

Table 2 Mutational concordance rate between tissue and cell-free DNA sample analysis

| | With MB | Without MB | |
|------------------|---------|------------|------|
| MAF cut-off, % | 0.2 | 0.5 | 10 |
| Match rate, % | 78.6 | 78.6 | 17.9 |
| Mismatch rate, % | 0 | 18.2 | 0 |

MAF, mutant allele frequency; MB, molecular barcode.

low as 0.1%. Gene alterations, including CNVs, were detected in 16 samples (52%), whereas no gene fusions were detected. Detected CNVs included *CCND2*, *CCND3*, *CDK4*, *FGFR1*, and *MYC*, which could be useful in precision medicine as these genes are targets of molecular-targeted drugs.

Notably, the later the timing of blood sampling in the clinical course, the more alterations and higher MAFs detected in the cfDNA. Concurrent samples were obtained from five patients who had a strong tendency to increase MAFs in *KRAS* as the disease progressed, with additional gene amplifications such as

MYC, *CCND2*, *CCND3*, and *CDK4*. The clinical course of case 14 for which three liquid biopsies were available is shown in Figure 4. Liver metastases were detected by laparotomy in the 53-year-old female with pancreatic tail cancer. The liver metastasis had become visible on computed tomography with an increase in CA19-9. The MAFs in *KRAS* showed a steep increase from 0.7% in the first liquid biopsy (LB_1) before laparotomy to 8% together with *MYC* amplification in the second liquid biopsy (LB_2) before the first-line chemotherapy. The MAFs in *KRAS* increased further to 12.4% together with *MYC* and *CCND2* amplifications in the third liquid biopsy (LB_3) before the second-line chemotherapy.

Discussion

This study investigated the effect of MB for reducing sequence- or PCR-derived errors on analyzing low MAFs in cfDNA from liquid biopsy samples compared with gene alterations detected in tissue samples. NGS analysis with MB could eliminate sequence- or PCR-derived errors, which enabled detection of accurate gene alterations with MAFs as low as 0.2%. Moreover,

Table 3 Gene alterations detected in cfDNA by dNGS compared with those detected by EUS-FNA

| Case | Tumor stage | Timing | Tissue [†] | cfDNA | | dNGS | | | | | | | | | |
|------|-------------|--------|---------------------|-------|--------------------------|------------|-------------------|------|---------|--------|------------|--------------------------|---------|--------------|--|
| | | | | NGS | Digital PCR [‡] | Mutations | | | | | | CNVs | | | |
| | | | | | | Main genes | MAF (%) | KRAS | | TP53_1 | | TP53_2 | | Gained genes | |
| | | | | | | | | AA | MAF (%) | AA | MAF (%) | AA | MAF (%) | | |
| 1 | 4 | D | <i>KRAS_G12D</i> | 3.0 | G12D | 2.4 | R282W | 2.3 | | | | | | | |
| 2 | 3 | D | <i>KRAS_G12R</i> | 1.2 | G12R | 0.5 | | | | | | | | | |
| 3 | 2 | D | <i>KRAS_G12V</i> | 2.3 | | | P301fs | 0.2 | | | | | | | |
| 4 | 4 | D | <i>KRAS_G12D</i> | 2.1 | | | | | | | | <i>CCND3</i> <i>CDK4</i> | | | |
| | | D | <i>KRAS_G12D</i> | 3.4 | | | | | | | | | | | |
| 5 | 3 | D | <i>KRAS_G12D</i> | 1.5 | | | | | | | | | | | |
| | | D | <i>KRAS_G12D</i> | 1.9 | G12D | 1.5 | R175H | 2.2 | S366fs | 0.1 | | | | | |
| 6 | 4 | P | <i>KRAS_G12D</i> | 2.3 | | | | | | | | | | | |
| 7 | 4 | P | <i>KRAS_G12V</i> | 7.6 | | | | | | | | | | | |
| 8 | 4 | P | <i>KRAS_G12D</i> | 10.5 | G12D | 9.3 | | | | | | | | | |
| 9 | 2 | P | <i>KRAS_G12D</i> | 10.4 | | | | | | | | | | | |
| 10 | 3 | P | <i>KRAS_G12V</i> | 4.5 | | | | | | | | | | | |
| 11 | 4 | P | <i>KRAS_G12V</i> | 6.0 | | | | | | | | | | | |
| 12 | 4 | P | <i>KRAS_G12D</i> | 6.8 | | | M237V | 0.4 | | | | | | | |
| 13 | 2 | P | <i>GNAS_R201C</i> | 10.4 | | | | | | | | | | | |
| 14 | 4 | P | <i>KRAS_G12D</i> | 1.6 | | | | | | | | | | | |
| | | D | <i>KRAS_G12D</i> | 41.4 | G12D | 38.7 | | | | | | | | | |
| 15 | 4 | P | <i>KRAS_G12R</i> | 2.5 | G12R | 0.7 | | | | | | | | | |
| | | D | <i>KRAS_G12R</i> | 12.0 | G12R | 8.0 | R273C | 4.8 | | | | <i>MYC</i> | | | |
| 16 | 2 | D | <i>KRAS_G12R</i> | 15.3 | G12R | 12.4 | R273C | 8.2 | | | | <i>MYC</i> <i>CCND2</i> | | | |
| | | P | <i>KRAS_G12V</i> | 7.3 | G12V | 1.3 | | | | | | | | | |
| 17 | 4 | P | <i>KRAS_G12V</i> | 16.3 | | | | | | | | | | | |
| 18 | 4 | P | <i>KRAS_G12V</i> | 7.5 | G12V | 7.2 | | | | | | | | | |
| 19 | 4 | P | <i>KRAS_G12D</i> | 42.1 | G12D | 37.1 | A159V | 24.5 | V274fs | 0.1 | <i>MYC</i> | <i>FGFR1</i> | | | |
| 20 | 4 | P | <i>KRAS_G12R</i> | 1.9 | G12R | 1.4 | C176 [§] | 1.0 | | | | | | | |
| 21 | 4 | P | <i>KRAS_G12V</i> | 8.8 | | | | | | | | | | | |
| | | P | <i>KRAS_G12V</i> | 7.1 | G12V | 8.2 | | | | | | | | | |
| 22 | 4 | P | <i>KRAS_G12V</i> | 9.9 | G12V | 10.6 | | | | | | | | | |
| | | P | <i>KRAS_G12V</i> | 4.0 | | | | | | | | | | | |
| 23 | 2 | P | <i>KRAS_G12R</i> | 2.5 | | | | | | | | | | | |
| 24 | 2 | P | <i>KRAS_G12V</i> | 5.5 | | | | | | | | | | | |

[†]Samples obtained by EUS-FNA.

[‡]Digital PCR was performed on gene mutations obtained in tissues.

[§]Stop codon.

AA, amino acid; cfDNA, cell-free DNA; CNVs, copy number variations; D, during therapy; dNGS, digital next-generation sequencing; EUS-FNA, endoscopic ultrasound-guided fine-needle aspiration; fs, frame shift; MAF, mutant allele frequency; P, pretherapy; PCR, polymerase chain reaction.

concurrent sampling enabled adding gene amplifications, which would be targeted by molecular-targeted drugs.

dNGS using MB could suppress sequence-/PCR-derived errors, enabling accurate diagnosis of gene alterations with very low MAFs in cfDNA. dNGS has been reported to be highly sensitive for gene mutations with low allele frequency.^{34,39,40} Recently, NGS was performed using the original DNA divided into 96 aliquots, enabling the detection of true variants if the same variants existed in different aliquots.⁴⁰ Another method used MB consisting of 12–14 nucleotides, which were attached

to the DNA in the first PCR step. Variants that exist throughout the same MB were considered true variants.^{34,39} These methods are useful for detecting low-abundant mutations in liquid biopsy samples; however, because only a few studies have compared variants that were detected in liquid biopsy samples with reference data,⁴¹ such as data on variants detected in tumor tissue, the accuracy of the method using clinical samples remains unclear. Although a recent study provided a comparison of variants in sequence reads obtained from plasma samples with and without MB using tissue-derived gene alterations as references,⁴¹ the

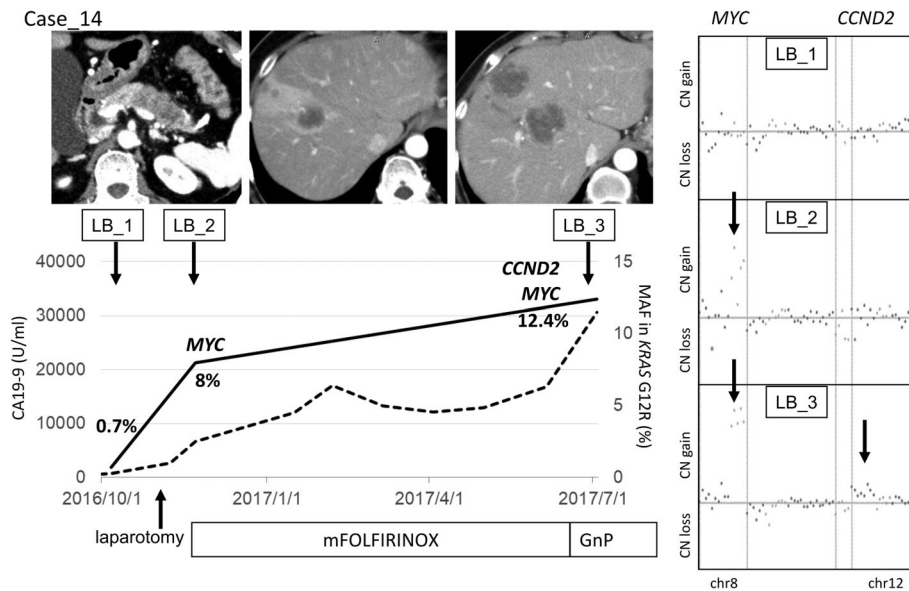


Figure 4 Clinical course of a representative case during systemic chemotherapy. Changes in tumor marker CA19-9 levels and mutant allele frequency (MAF) are shown as dotted and solid line graphs, respectively, and representative computed tomography images are displayed in the upper panel. In this case, liquid biopsies were obtained three times during the clinical course from which copy number alterations (CNAs) of cell-free DNA together with gene mutations were analyzed. The right panels show CNAs in *MYC* and *CCND2* as dot plots, in which dots elevated from the center line correspond with amplified genes (arrows).

sequence reads with or without MBs from plasma samples were different and were analyzed using a different algorithm, and the authors could not detect low-abundant mutations in sequence reads without MB. In this study, tissue-derived variants were also used as references. Furthermore, we compared the analysis with and without MB using the same sequence reads from plasma samples. Our study clarified that the analysis without MB enabled the diagnosis of low-abundant mutations together with many erroneous variants, which, however, were eliminated when the analysis was performed with MB. Therefore, we conclude that NGS using MBs enables the detection of low-abundant mutations with high accuracy.

The findings of this study have multiple clinical implications. First, liquid biopsy using MB could allow for the development of more treatment options. Because liquid biopsy using dPCR can detect MAFs as low as 0.1%, it is almost ready for application. For example, the EGFR-T790M mutation, which is the alteration that is most frequently associated with anti-Epidermal growth factor receptor (EGFR) tyrosine kinase inhibitor resistance, can be detected in cfDNA as an alternative to the detection of tumor DNA in tissue sample in patients with metastatic non-small cell lung cancer, and a designated test kit has already been implemented for clinical use.⁴² Moreover, efficient diagnosis of mutations in *KRAS*, *BRAF*, *NRAS*, and *PIK3CA* by liquid biopsy using MB can be used to map and monitor the resistance toward molecular-targeted drugs, which are widely used in conjunction with systemic chemotherapy in colorectal cancer.⁴³ However, currently, dPCR can only detect a limited number of mutations that are already known, which makes it applicable to only a limited number of cancer types. Nevertheless, dNGS that has overcome sequence- and PCR-derived errors

is expected to broaden the indication for liquid biopsy. Second, liquid biopsy is less invasive than tissue biopsy,⁴⁴ which makes it feasible to obtain a genetic profile of the tumor on a repetitive basis, even in patients with advanced cancer, increasing the possibility of detecting cancer-related gene mutations, including gene mutations that could be potential drug molecular targets. Indeed, in our study, data obtained using liquid biopsy revealed additional gene amplifications, such as *CCND2*, *CCND3*, *CDK4*, *FGFR1*, and *MYC*, which could be targets for molecular-targeted drugs (Table 3 and Fig. 4). Third, liquid biopsy using MBs provided more genetic information than that obtained from tissues with high accuracy, which would increase our understanding of within-tumor genetic heterogeneity. Recent multiregion sequencing of tumor tissue demonstrated tumor heterogeneity as a consequence of clonal evolution.^{45–48} Because tissue biopsy has important limitations such as invasiveness and incomplete capture of tumor heterogeneity,⁴⁴ error-suppressed dNGS on material obtained by liquid biopsy would help in the understanding of cancer biology.

This study has several limitations. First, the design was retrospective, and only a small number of cases was recruited from a single center. Second, the gene panel employed targeted several gene fusions, which could not be detected in this study. The reason why we could not detect gene fusions was partly due to insufficient preservation of plasma samples. The samples were stored at -20°C , not at -80°C , which might have affected our results. Third, the detectability of gene mutation in dNGS seemed to be lower than that expected. Given the successful detection of gene mutation by dPCR using similar amounts of cfDNA (as shown in Table 3), we thought that the cause of insufficient sensitivity in dNGS could be a technical issue in sequencing.

The molecular depth in dNGS needed was as large as 1500 or 3000 per sample to detect MAFs as low as 0.2% or 0.1%, respectively, because the analysis setting required a minimum of three identical reads to identify a mutation. However, the average and median molecular depths in our study were 793 and 536, respectively, and the average and median read depths were 18 509 and 12 321, respectively (Table S3), suggesting the cause to be insufficient molecular depths. To improve molecular depths, two- or threefold greater sequence read depths than those obtained in this study would be required, which we plan on accomplishing in future studies.

In conclusion, we proved liquid biopsy-derived cfDNA using dNGS to be accurate by direct comparison of sequence reads with and without MB together using gene alterations detected in tumor tissue as a reference. We believe that these findings will help the scientific community improve the detection of molecular-targetable genes using liquid biopsy, even in patients whose physical strength has significantly declined owing to cancer progression.

Acknowledgments

This study was supported by grants from the Japan Society for the Promotion of Science (JSPS KAKENHI grant numbers 19K08418, 18K07999, and 15K09044; <http://www.jps.go.jp/j-grantsinaid/>). We thank Takako Ohmori and Tomoko Nakajima for their valuable technical assistance and Masato Takano (Orange Square) for his computer programming assistance. We thank Enago (www.enago.jp) for the English language review.

References

- Vogelzang NJ, Benowitz SI, Adams S *et al.* Clinical cancer advances 2011: annual report on progress against cancer from the American Society of Clinical Oncology. *J. Clin. Oncol.* 2012; **30**: 88–109.
- Nakagawa-Senda H, Yamaguchi M, Matsuda T *et al.* Cancer prevalence in Aichi, Japan for 2012: estimates based on incidence and survival data from population-based cancer registry. *Asian Pac. J. Cancer Prev.* 2017; **18**: 2151–6.
- Lee YT, Tan YJ, Oon CE. Molecular targeted therapy: treating cancer with specificity. *Eur. J. Pharmacol.* 2018; **834**: 188–96.
- Shin HJ, Lahoti S, Sneige N. Endoscopic ultrasound-guided fine-needle aspiration in 179 cases: the M. D. Anderson Cancer Center experience. *Cancer.* 2002; **96**: 174–80.
- Forshew T, Murtaza M, Parkinson C *et al.* Noninvasive identification and monitoring of cancer mutations by targeted deep sequencing of plasma DNA. *Sci. Transl. Med.* 2012; **4**: 136ra68.
- Diehl F, Schmidt K, Choti MA *et al.* Circulating mutant DNA to assess tumor dynamics. *Nat. Med.* 2008; **14**: 985–90.
- Lo YM, Zhang J, Leung TN, Lau TK, Chang AM, Hjelm NM. Rapid clearance of fetal DNA from maternal plasma. *Am. J. Hum. Genet.* 1999; **64**: 218–24.
- Bidard FC, Kiavue N, Ychou M *et al.* Circulating tumor cells and circulating tumor DNA detection in potentially resectable metastatic colorectal cancer: a prospective ancillary study to the Unicancer Prodigé-14 trial. *Cells.* 2019; **8** (6): 516.
- Onidani K, Shoji H, Kakizaki T *et al.* Monitoring of cancer patients via next-generation sequencing of patient-derived circulating tumor cells and tumor DNA. *Cancer Sci.* 2019; **110**: 2590–9.
- Tan CR, Zhou L, El-Deiry WS. Circulating tumor cells versus circulating tumor DNA in colorectal cancer: pros and cons. *Curr. Colorectal. Cancer Rep.* 2016; **12**: 151–61.
- Shimomura A, Shiino S, Kawauchi J *et al.* Novel combination of serum microRNA for detecting breast cancer in the early stage. *Cancer Sci.* 2016; **107**: 326–34.
- Yokoi A, Matsuzaki J, Yamamoto Y *et al.* Integrated extracellular microRNA profiling for ovarian cancer screening. *Nat. Commun.* 2018; **9**: 4319.
- Usuba W, Urabe F, Yamamoto Y *et al.* Circulating miRNA panels for specific and early detection in bladder cancer. *Cancer Sci.* 2018; **110**: 408–19.
- Liebs S, Keilholz U, Kehler I, Schweiger C, Haybäck J, Nonnenmacher A. Detection of mutations in circulating cell-free DNA in relation to disease stage in colorectal cancer. *Cancer Med.* 2019; **8**: 3761–9.
- Furuki H, Yamada T, Takahashi G *et al.* Evaluation of liquid biopsies for detection of emerging mutated genes in metastatic colorectal cancer. *Eur. J. Surg. Oncol.* 2018; **44**: 975–82.
- Zhang H, Liu R, Yan C *et al.* Advantage of next-generation sequencing in dynamic monitoring of circulating tumor DNA over droplet digital PCR in cetuximab treated colorectal cancer patients. *Transl. Oncol.* 2019; **12**: 426–31.
- Thomsen CB, Andersen RF, Lindebjerg J, Hansen TF, Jensen LH, Jakobsen A. Plasma dynamics of RAS/RAF mutations in patients with metastatic colorectal cancer receiving chemotherapy and anti-EGFR treatment. *Clin. Colorectal. Cancer.* 2019; **18**: 28–33.e3.
- Osumi H, Shinozaki E, Takeda Y *et al.* Clinical relevance of circulating tumor DNA assessed through deep sequencing in patients with metastatic colorectal cancer. *Cancer Med.* 2019; **8**: 408–17.
- Yang YC, Wang D, Jin L *et al.* Circulating tumor DNA detectable in early- and late-stage colorectal cancer patients. *Biosci. Rep.* 2018; **38** (4): BSR20180322.
- Sun Q, Liu Y, Liu B, Liu Y. Use of liquid biopsy in monitoring colorectal cancer progression shows strong clinical correlation. *Am. J. Med. Sci.* 2018; **355**: 220–7.
- Normanno N, Esposito Abate R, Lambiase M *et al.* RAS testing of liquid biopsy correlates with the outcome of metastatic colorectal cancer patients treated with first-line FOLFIRI plus cetuximab in the Capri-GOIM trial. *Ann. Oncol.* 2018; **29**: 112–18.
- Vidal J, Muinelo L, Dalmases A *et al.* Plasma ctDNA RAS mutation analysis for the diagnosis and treatment monitoring of metastatic colorectal cancer patients. *Ann. Oncol.* 2017; **28**: 1325–32.
- Yamada T, Iwai T, Takahashi G *et al.* Utility of KRAS mutation detection using circulating cell-free DNA from patients with colorectal cancer. *Cancer Sci.* 2016; **107**: 936–43.
- Rachiglio AM, Esposito Abate R, Sacco A *et al.* Limits and potential of targeted sequencing analysis of liquid biopsy in patients with lung and colon carcinoma. *Oncotarget.* 2016; **7**: 66595–605.
- Takeda K, Yamada T, Takahashi G *et al.* Analysis of colorectal cancer-related mutations by liquid biopsy: utility of circulating cell-free DNA and circulating tumor cells. *Cancer Sci.* 2019; **110**: 3497–509.
- Sun X, Huang T, Cheng F *et al.* Monitoring colorectal cancer following surgery using plasma circulating tumor DNA. *Oncol. Lett.* 2018; **15**: 4365–75.
- Reinert T, Henriksen TV, Christensen E *et al.* Analysis of plasma cell-free DNA by ultradeep sequencing in patients with stages I to III colorectal cancer. *JAMA Oncol.* 2019; **5**: 1124–31.
- Shen SY, Singhanian R, Fehringer G *et al.* Sensitive tumour detection and classification using plasma cell-free DNA methylomes. *Nature.* 2018; **563**: 579–83.
- Mair R, Mouliere F, Smith CG *et al.* Measurement of plasma cell-free mitochondrial tumor DNA improves detection of glioblastoma in patient-derived orthotopic xenograft models. *Cancer Res.* 2019; **79**: 220–30.

- 30 Mouliere F, Chandrananda D, Piskorz AM *et al.* Enhanced detection of circulating tumor DNA by fragment size analysis. *Sci. Transl. Med.* 2018; **10**: 466.
- 31 Ono Y, Sugitani A, Karasaki H *et al.* An improved digital polymerase chain reaction protocol to capture low-copy KRAS mutations in plasma cell-free DNA by resolving “subsampling” issues. *Mol. Oncol.* 2017; **11**: 1448–58.
- 32 Takai E, Totoki Y, Nakamura H *et al.* Clinical utility of circulating tumor DNA for molecular assessment in pancreatic cancer. *Sci. Rep.* 2015; **5**: 18425.
- 33 Alcaide M, Yu S, Davidson J *et al.* Targeted error-suppressed quantification of circulating tumor DNA using semi-degenerate barcoded adapters and biotinylated baits. *Sci. Rep.* 2017; **7**: 10574.
- 34 Ståhlberg A, Krzyzanowski PM, Jackson JB, Egyud M, Stein L, Godfrey TE. Simple, multiplexed, PCR-based barcoding of DNA enables sensitive mutation detection in liquid biopsies using sequencing. *Nucleic Acids Res.* 2016; **44**: e105.
- 35 Newman AM, Lovejoy AF, Klass DM *et al.* Integrated digital error suppression for improved detection of circulating tumor DNA. *Nat. Biotechnol.* 2016; **34**: 547–55.
- 36 Schmitt MW, Kennedy SR, Salk JJ, Fox EJ, Hiatt JB, Loeb LA. Detection of ultra-rare mutations by next-generation sequencing. *Proc. Natl. Acad. Sci. U.S.A.* 2012; **109**: 14508–13.
- 37 Takano S, Fukasawa M, Kadokura M *et al.* Next-generation sequencing revealed TP53 mutations to be malignant marker for intraductal papillary mucinous neoplasms that could be detected using pancreatic juice. *Pancreas.* 2017; **46**: 1281–7.
- 38 Forbes SA, Bindal N, Bamford S *et al.* COSMIC: mining complete cancer genomes in the Catalogue of Somatic Mutations in Cancer. *Nucleic Acids Res.* 2011; **39**: D945–50.
- 39 Kinde I, Wu J, Papadopoulos N, Kinzler KW, Vogelstein B. Detection and quantification of rare mutations with massively parallel sequencing. *Proc. Natl. Acad. Sci. U.S.A.* 2011; **108**: 9530–5.
- 40 Yu J, Sadakari Y, Shindo K *et al.* Digital next-generation sequencing identifies low-abundance mutations in pancreatic juice samples collected from the duodenum of patients with pancreatic cancer and intraductal papillary mucinous neoplasms. *Gut.* 2017; **66**: 1677–87.
- 41 Hirotsu Y, Otake S, Ohyama H *et al.* Dual-molecular barcode sequencing detects rare variants in tumor and cell free DNA in plasma. *Sci. Rep.* 2020; **10**: 3391.
- 42 Mok T, Wu YL, Lee JS *et al.* Detection and dynamic changes of EGFR mutations from circulating tumor DNA as a predictor of survival outcomes in NSCLC patients treated with first-line intercalated erlotinib and chemotherapy. *Clin. Cancer Res.* 2015; **21**: 3196–203.
- 43 De Roock W, Claes B, Bernasconi D *et al.* Effects of KRAS, BRAF, NRAS, and PIK3CA mutations on the efficacy of cetuximab plus chemotherapy in chemotherapy-refractory metastatic colorectal cancer: a retrospective consortium analysis. *Lancet Oncol.* 2010; **11**: 753–62.
- 44 Russano M, Napolitano A, Ribelli G *et al.* Liquid biopsy and tumor heterogeneity in metastatic solid tumors: the potentiality of blood samples. *J. Exp. Clin. Cancer Res.* 2020; **39**: 1–13.
- 45 Yachida S, Jones S, Bozic I *et al.* Distant metastasis occurs late during the genetic evolution of pancreatic cancer. *Nature.* 2010; **467**: 1114–17.
- 46 von Loga K, Woolston A, Punta M *et al.* Extreme intratumour heterogeneity and driver evolution in mismatch repair deficient gastro-oesophageal cancer. *Nat. Commun.* 2020; **11**: 1–14.
- 47 Yan T, Cui H, Zhou Y *et al.* Multi-region sequencing unveils novel actionable targets and spatial heterogeneity in esophageal squamous cell carcinoma. *Nat. Commun.* 2019; **10**: 1670.
- 48 Hu X, Fujimoto J, Ying L *et al.* Multi-region exome sequencing reveals genomic evolution from preneoplasia to lung adenocarcinoma. *Nat. Commun.* 2019; **10**: 2978.

Supporting information

Additional supporting information may be found in the online version of this article at the publisher’s website:

Table S1. Genes assayed in tissues by digital next-generation sequencing.

Table S2. Genes assayed in cell-free DNA by digital next-generation sequencing.

Table S3. Coverage analyses of digital next-generation sequencing.